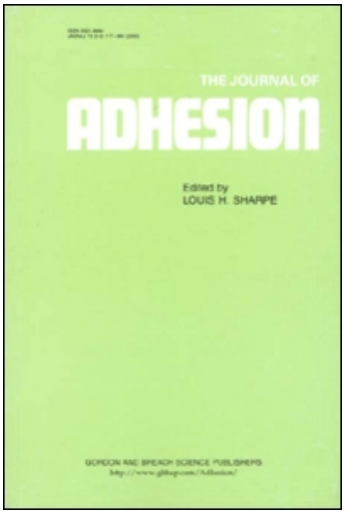

The Journal of Adhesion
Publication details, including instructions for authors and subscription information:
http://www.informaworld.com/smpp/title~content=t713453635

Durability Testing of Epoxy Adhesive Bonds

D. R. Arnott[a]; M. R. Kindermann[a]
[a] Airframes and Engines Division, Aeronautical and Maritime Research Laboratory, Defence Science and Technology Organisation, Melbourne, Australia

To cite this Article Arnott, D. R. and Kindermann, M. R.(1995) 'Durability Testing of Epoxy Adhesive Bonds', The Journal of Adhesion, 48: 1, 101 — 119
To link to this Article: DOI: 10.1080/00218469508028157
URL: http://dx.doi.org/10.1080/00218469508028157

J. Adhesion, 1995, Vol. 48, pp. 101–119
Reprints available directly from the publisher
Photocopying permitted by license only

Durability Testing of Epoxy Adhesive Bonds

D. R. ARNOTT and M. R. KINDERMANN

Defence Science and Technology Organisation, Airframes and Engines Division, Aeronautical and Maritime Research Laboratory, 506 Lorimer St., Fishermen's Bend, Melbourne 3207, Australia

(Received November 18, 1993; in final form May 24, 1994)

Epoxy adhesive bond durabilities were estimated by a constant displacement-rate method, based on both elastic energy release rate, G_1, and crack velocity. Tests conducted in humid air at 50 °C on adhesively-bonded aluminium alloy showed that G_1 depended strongly on load-point displacement-rate. The fracture energy of undegraded bonds, G_{1C}, the fracture energy for degraded bonds, G_{1SCC}, and a bond durability indicator, v_g, were each determined. G_{1C} was higher for grit-blasted adherends anodized in phosphoric acid than for grit-blasted adherends treated with a silane coupling agent solution (SCA). Grit-blasted adherends treated with SCA formed more durable bonds than those anodised in phosphoric acid. X-ray photolectron spectroscopy of fracture surfaces on SCA-treated adherends indicated that humidity had degraded the oxide film. Fracture surface inspection indicated that total adhesive failure did not necessarily imply low fracture toughness. This was explained in terms of a "plastic expansion" model.

KEY WORDS Adhesive bond; epoxy film adhesive; aluminium alloy; accelerated durability testing.

INTRODUCTION

The field repair of aircraft components with structural adhesives imposes different requirements to those arising during manufacture. The minimum surface treatment of adherends and minimum cure of adhesives to achieve appropriate bond strength is now used for field repairs.[1,2] The preparation of bonds under minimum conditions places an emphasis on the need for quantitative evaluations of strength, fracture toughness and durability. These requirements have stimulated the development of the constant displacement-rate test (CDRT).[3,4]

The specimen used in the CDRT is similar to that used in the Boeing wedge test.[5] The ranking of bond durability using the Boeing wedge test has been shown to correlate with service experience and was found more reliable than the conventional lap-shear or peel tests.[6]

1.1 Constant Displacement-rate Test

The CDRT described previously[3,4] allows the determination of elastic energy release rates, G_1, for a wide range of defined crack growth rates.

1.1.1 Elastic Energy Release Rate In the CDRT, the specimen shown in Figure 1 is opened at a constant load-point displacement-rate. The load-point displacement, w, and resulting load, P, are measured during the test. The elastic energy release rate, G_1, is calculated from equation (1):[3,4]

$$w = \left[\frac{Eh^3 G_1^3 b^4}{27}\right]^{1/2} \frac{1}{P^2} \tag{1}$$

Where E is the Young's modulus, h the thickness and b the width of the adherends. Equation (1) is valid provided that the crack length is much greater than the adherend thickness[7,8] and plastic deformation in the adherends is negligible.[4]

1.1.2 Crack Velocity The crack velocity, dl/dt, is related to the load-point displacement-rate, dw/dt, as shown by equation (2):[4]

$$\frac{dl}{dt} = \frac{3}{4b}\left(\frac{P}{G_1}\right)\frac{dw}{dt} \tag{2}$$

The crack velocity, dl/dt, and the load, P, both decrease as the test progresses at constant dw/dt. However, the variation in dl/dt in one test is quite small when compared with the range in crack velocity of 10^3 used in this series of tests.[3,4]

1.1.3 G_{1C}, G_{1SCC}, v_g A series of constant displacement-rate tests were conducted on specimens of grit-blasted 2024-T3 clad aluminium alloy, bonded with AF126[a] epoxy

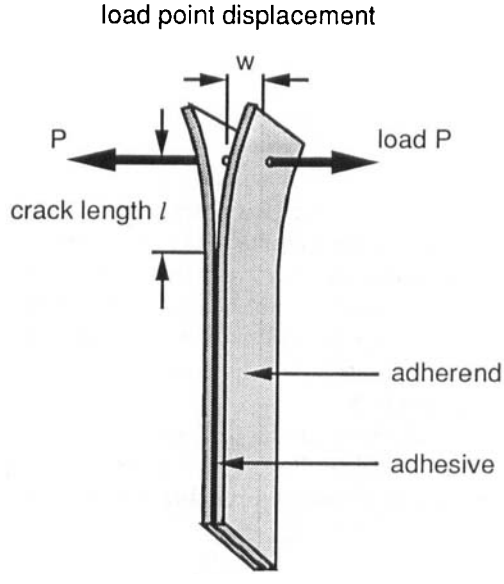

FIGURE 1 Bonded double-cantilever-beam specimen used in the constant displacement-rate test.

[a] Minnesota Mining and Manufacturing Company (3M).

adhesive. These tests showed that there are one or more linear segments[3,4] in almost all plots of w *versus* P^{-2}. G_1 values can be determined for each linear segment from the gradient of this plot using equation (1).

Tests conducted on these specimens in saturated humidity at 50°C show that G_1 depends strongly on crack velocity, dl/dt (Figure 2). At high values of dl/dt, G_1 is equal to the critical fracture energy of the undergraded bond, G_{1C}^4. At very low values of dl/dt, water vapour degrades the bond ahead of the crack tip and G_1 becomes the fracture energy of the fully degraded bond, G_{1SCC}. Between these extremes, G_1 is sensitive to crack velocity (or load-point displacement-rate) because water vapour degrades the bond at a rate similar to the crack velocity.

Crack velocity is sensitive to the degradation rate of the bond ahead of the crack tip. A fast crack advances into material that has had insufficient time to be degraded by water vapour, whereas a slow crack advances into degraded material. The degree of degradation will depend on the time available for water vapour to diffuse into the bond ahead of the crack front where it can act on the interfacial oxide or polymer bonds. Bond durability can be estimated by focussing on the range of crack velocity where G_1 decreases rapidly as the crack velocity is decreased. The transitional crack velocity, v_{trans}, calculated from values within the transition region shown in Figure 2, represents the equilibrium between the rate of bond degradation and the rate of crack advance.[4] This v_{trans} can be used as a bond durability indicator for comparing adherend treatments. The velocity, V_g, is a graphical estimate of the mean crack velocity taken from a best fit plot of G_1 *versus* dl/dt as shown in Figure 2 and approximates v_{trans}.

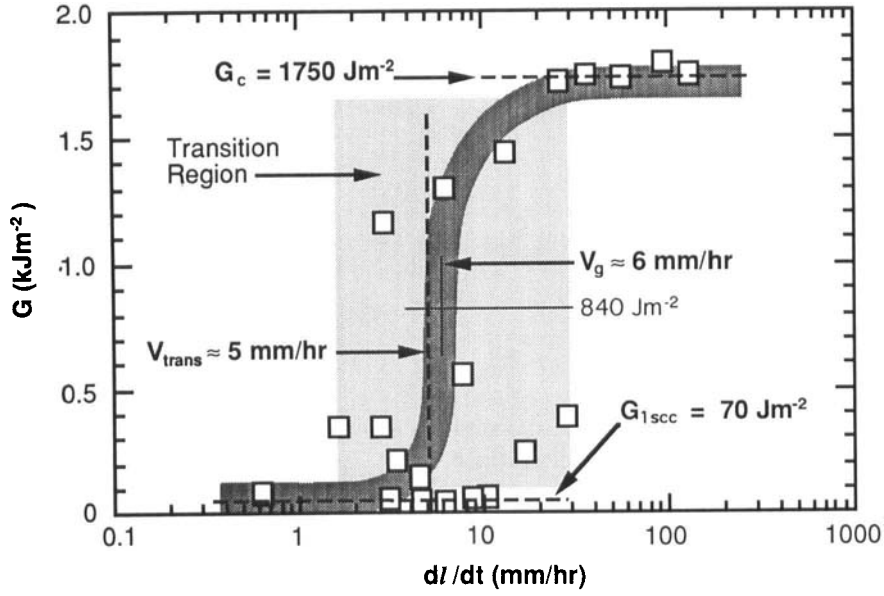

FIGURE 2 A plot of G_1 *versus* dl/dt showing v_{trans} and v_g. Adherends were grit-blasted. Specimens were tested in warm humid air.

1.2 Selection of Surface Treatments

The CDRT determines the influence of adherend surface treatment on the durability and fracture properties of bonded DCB specimens. An organo-functional coupling agent (SCA) formed part of the surface treatment, since this was known to improve the durability of the bond.[1,2,9] Phosphoric acid anodization (PAA) was chosen as a second surface treatment since it is also known to improve bond strength and durability.[10–12] The PAA treatment used here did not include the chromic acid etch used commercially and specified by the industry standard. There was no primer applied to the adherend surfaces.

1.3 Failure Mode

Visual examination of the adherends, separated at the conclusion of tests, provides some information on the mode of failure. A failure occuring in the body of the adhesive is known as a "cohesive" failure and one occurring at the metal-adhesive interface is known as an "adhesive" failure. In a "cohesive" failure, complementary areas on fracture surfaces of each adherend have the appearance of epoxy resin.

In an "adhesive" failure, an examination of the fracture surfaces of the two adherends show complementary areas having different appearances. Areas on one adherend have a "metallic" appearance, whilst corresponding areas on the other adherend has the appearance of the epoxy adhesive. Inspection of both adherends is essential, as the fracture may meander between the two adherend surfaces.

The "metallic appearance fraction" or MAF is defined as the ratio of the sum of all areas on both mating adherends with a metallic appearance to the total fracture surface area. Thus, for a total "adhesive" failure the MAF = 0.5 and for a total cohesive failure the MAF = 0.

A "metallic" appearance on a fracture surface does not necessarily indicate "adhesive" failure. Voids penetrating to the adherend surface can result in areas of "metallic" appearance. It is very difficult to distinguish between small voids and small areas of "adhesive" failure.

Results of visual inspections of adherends are presented here as a "metallic appearance fraction" (MAF). Interpretation of this data in terms of "cohesive" failure, "adhesive" failure and void content is considered separately.

2 EXPERIMENTAL

Plates of 2024-T3 clad aluminium alloy (152.4 × 152.4 × 3.2 mm) were machined to receive hemispherical-headed loading screws.[4] These plates were grouped according to one of the following three surface treatments;

(i) **Grit-blast**: plates were degreased with AR grade methylethylketone, abraded with a dry Nylon scouring pad (Scotch-Brite®[a]) and cleaned with pressurised dry

[a] Minnesota Mining and Manufacturing Company (3M).

nitrogen. They were then grit-blasted with 50-micron alumina and cleaned again with pressurised dry nitrogen.[4]

(ii) **Grit-blast plus SCA:** plates were grit-blasted as in (i) above and then immersed for ten minutes in an aqueous solution of a silane coupling agent[b3]. These plates were dried in a stream of dry nitrogen prior to bonding.

(iii) **Grit-blast plus PAA:** plates were grit-blasted as in (i) above and anodized in a 12% *v/v* aqueous phosphoric acid solution. The potential was raised to 6 volts in increments of 1 volt at 1 minute intervals and held for 10 minutes. The plates were rinsed in distilled water and dried in a stream of dry nitrogen prior to bonding. This is not the commercial Phosphoric Acid Anodization treatment which incorporates a chromic acid etch prior to anodization.[10–12]

Paired plates with loading screws installed were bonded with AF126[a] film adhesive as described in a previous paper.[4] Five DCB specimens were cut and machined from the bonded plates.

The specimens were heated to 50°C and tested with dw/dt ranging from 50 mm/hr to 5 μm/hr. Some specimens were tested in dry air and the remaining in saturated humidity. A foil cover was placed over the upper end of the specimen to prevent condensed water accumulating in the crack. The load, P, and load-point displacement, w, were recorded at fixed intervals. G_1 was calculated from the gradient of a plot of w *versus* P^{-2} shown in equation (1). The crack velocity, dl/dt, was calculated using equation (2). Plastic bending of the adherends was negligible[4].

The fracture surfaces of specimens were examined both visually and with a video camera coupled to a Quick Capture®-Macintosh II®[c] image-processing system. Selected specimens were examined with a Surface Science Laboratories Model X-Probe SSX 100® X-ray photoelectron spectrometer using monochromatized Al Kα radiation and a probe size of 0.5 mm diameter[d].

3 RESULTS

3.1 Adherends with a Grit-Blast Treatment

Figure 3, curve (i), shows a plot of G_1 *versus* dw/dt for tests conducted in warm humid air on specimens with grit-blasted adherends. G_1 decreased from 1750 to 70 Jm^{-2} as dw/dt was decreased from 10 to 0.1 mm/hr. Figure 3, curve (i), also shows that G_1 is unstable within the dw/dt range of 0.2 to 3.6 mm/hr. G_1 was stable for both higher and lower load-point displacement rates.

Figure 4(a) shows a photograph of the fracture surfaces of a specimen tested at 3.6 mm/hr in warm dry air. Here, failure had occurred principally in the adhesive film. The mean value of the MAF was 0.25 ± 0.05 with regions of metallic appearance on both adherends, typically in small zones of 0.5 to 10 mm^2. Close examination of the fracture surfaces indicated that the void content was a small contribution to the MAF.

[a] Minnesota Mining and Manufacturing Company (3M).
[b] Union Carbide A-187.
[c] Registered Trade Marks of Data Translation and Apple Computer Incorporated, respectively.
[d] Conducted at Surface Science Laboratories 465 National Ave, Mountain View, CA, USA.

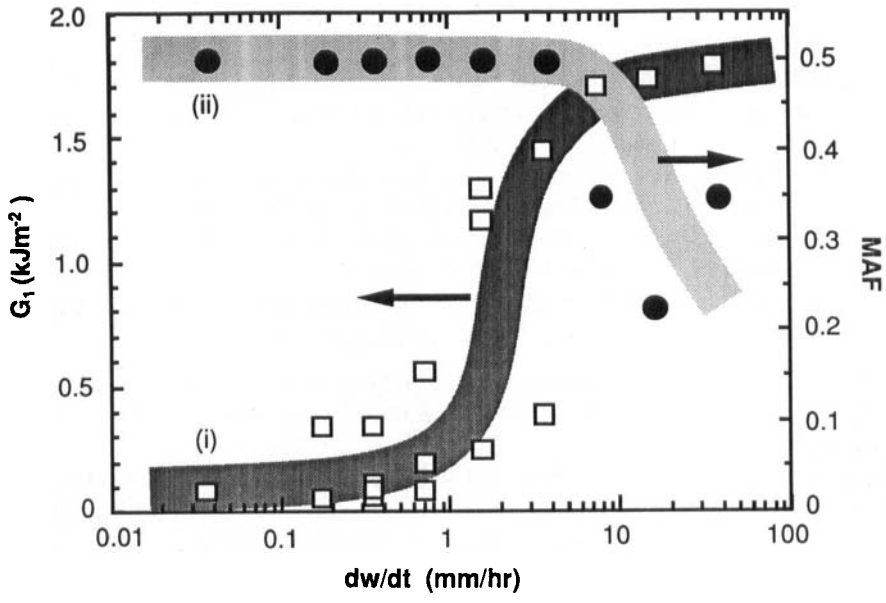

FIGURE 3 Plot of (i) G_1 and (ii) MAF *versus* dw/dt for specimens with grit-blasted adherends, tested in warm humid air. The arrows indicate the relevant reference scale.

There was no evidence of "plastic expansion" in the adhesive. "Plastic expansion" is defined as a mode of deformation where the adhesive stretches in response to adhesive failure in complementary regions on each adherend in a manner similar to that shown in Figure 4(d). Figure 4(a) was typical of specimens tested under dry conditions with dw/dt ranging from 36 to 0.36 mm/hr.

In Figure 3, curve (ii), the MAF had increased in warm humid air as dw/dt was decreased from 36 to 3.6 mm/hr. The fracture surface photographs in Figure 4(b) revealed two modes of failure for a specimen tested in warm humid air at a dw/dt of 36 mm/hr:

1. In the first mode, the failure was "adhesive". This failure was almost continuous near both edges of the specimen. The surface with "metallic" appearance was stained by exposure to water. The adhesive showed some evidence of plastic expansion.
2. In the second mode, the failure was near the longitudinal axis of other specimen and was similar to that described for the dry case (compare Figure 4(a) with 4(b)). Approximately one quarter of this failure surface had a "metallic" appearance.

The first failure mode clearly relates to the ingress of water into the adhesive bond during the test, whereas the second mode is characteristic of failure under dry conditions.

Figure 3, curve (ii), shows a MAF of 0.5 where dw/dt was less than 3.6 mm/hr in warm humid air. The failure shown in Figure 4(c) was "adhesive" and principally confined to

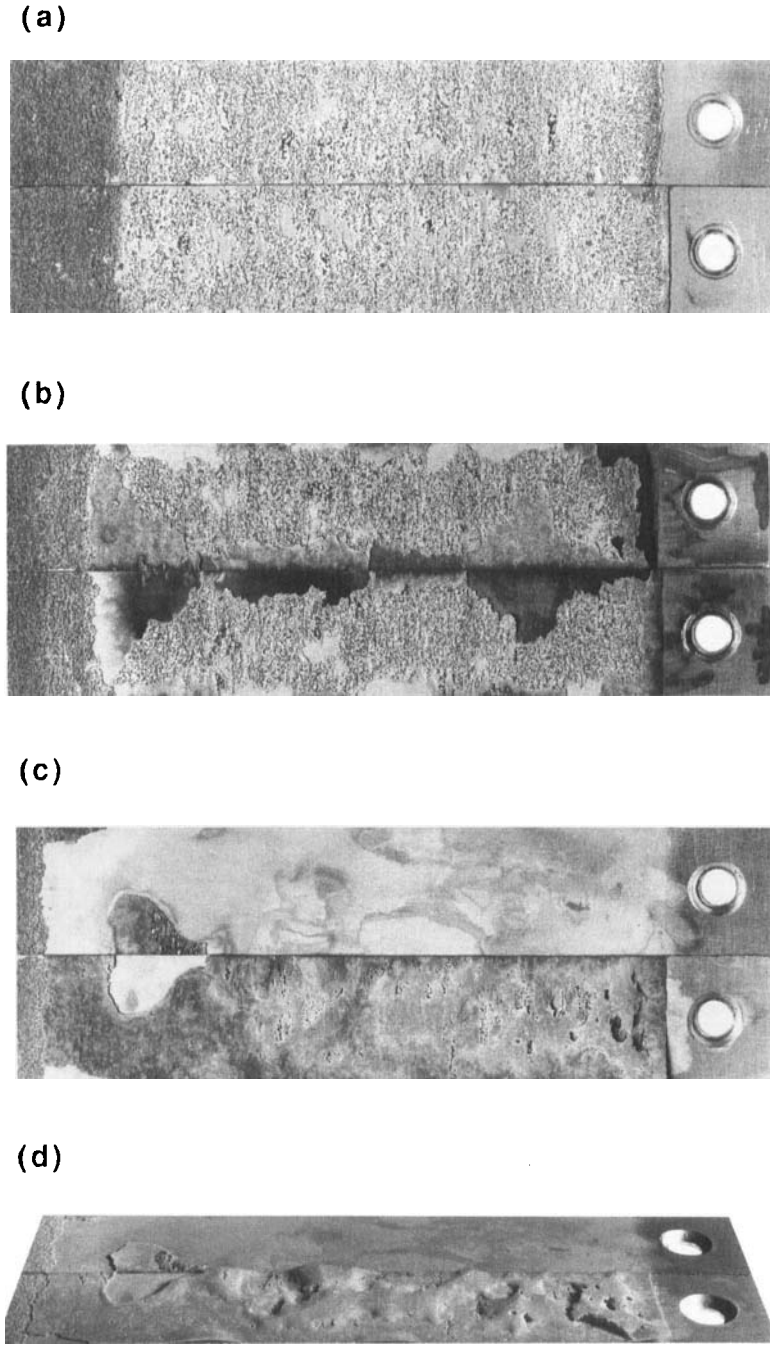

FIGURE 4 Photographs of three fracture surfaces between grit-blasted adherends, tested as follows;

(a) warm dry air, $dw/dt = 3.6$ mm/hr.
(b) warm humid air, $dw/dt = 36$ mm/hr.
(c) warm humid air, $dw/dt = 3.6$ mm/hr.
(d) warm humid air, $dw/dt = 3.6$ mm/hr showing plastic expansion of the adhesive.

one adherend surface. Figure 4(d) shows another view of the same specimen in which plastic expansion of the adhesive can be more clearly seen.

Figure 3 shows that "adhesive" failure does not necessarily imply greatly reduced fracture toughness. At a *dw/dt* of 3.6 mm/hr, the MAF of 0.5 indicated that failure was completely "adhesive", but the value of G_1 (1450 Jm^{-2}) is approximately 80% of the maximum value obtained for tests in warm dry air.

3.2 Adherends with a Grit-blast plus SCA Treatment

Figure 5, curve (i), shows a plot of G_1 *versus* *dw/dt* for tests conducted in warm humid air on specimens where the adherends were grit-blasted and treated with SCA solution. Water vapour caused both a large reduction and variability in G_1 where *dw/dt* was less than 0.36 mm/hr. For the nominally-dry case, both the reduction and variability in G_1 were minimal.

The photograph in Figure 6(a) shows the fracture surfaces of a specimen tested at 0.36 mm/hr in warm dry air. Again, failure had occurred principally in the adhesive film. The MAF was approximately 0.25 and distributed on both adherends, typically in small zones of 0.5 to 10 mm^2. Close examination of these fracture surfaces again indicated that the void content was a small contribution to the MAF. Plastic expansion of the adhesive was not apparent. Figure 6(a) was typical of specimens tested in warm dry air with *dw/dt* ranging from 3.6 to 0.015 mm/hr.

Figure 5, curve (ii), showed that the MAF had increased as *dw/dt* was decreased from 3.6 to 0.085 mm/hr for specimens tested in warm humid air. The photographs of the

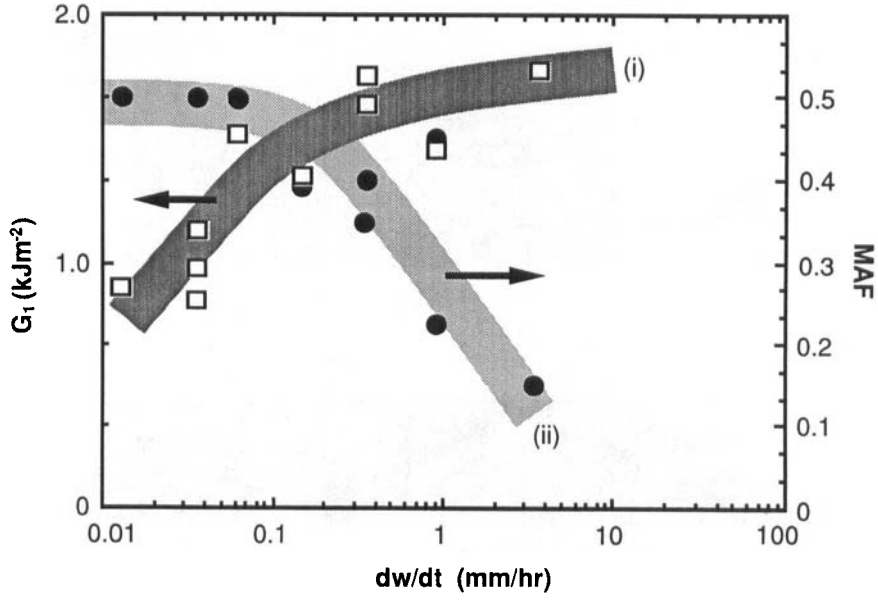

FIGURE 5 Plots of (i) G_1 and (ii) MAF *versus* *dw/dt* for specimens with grit-blast plus SCA treated adherends, tested in warm humid air. The arrows indicate the relevant reference scale.

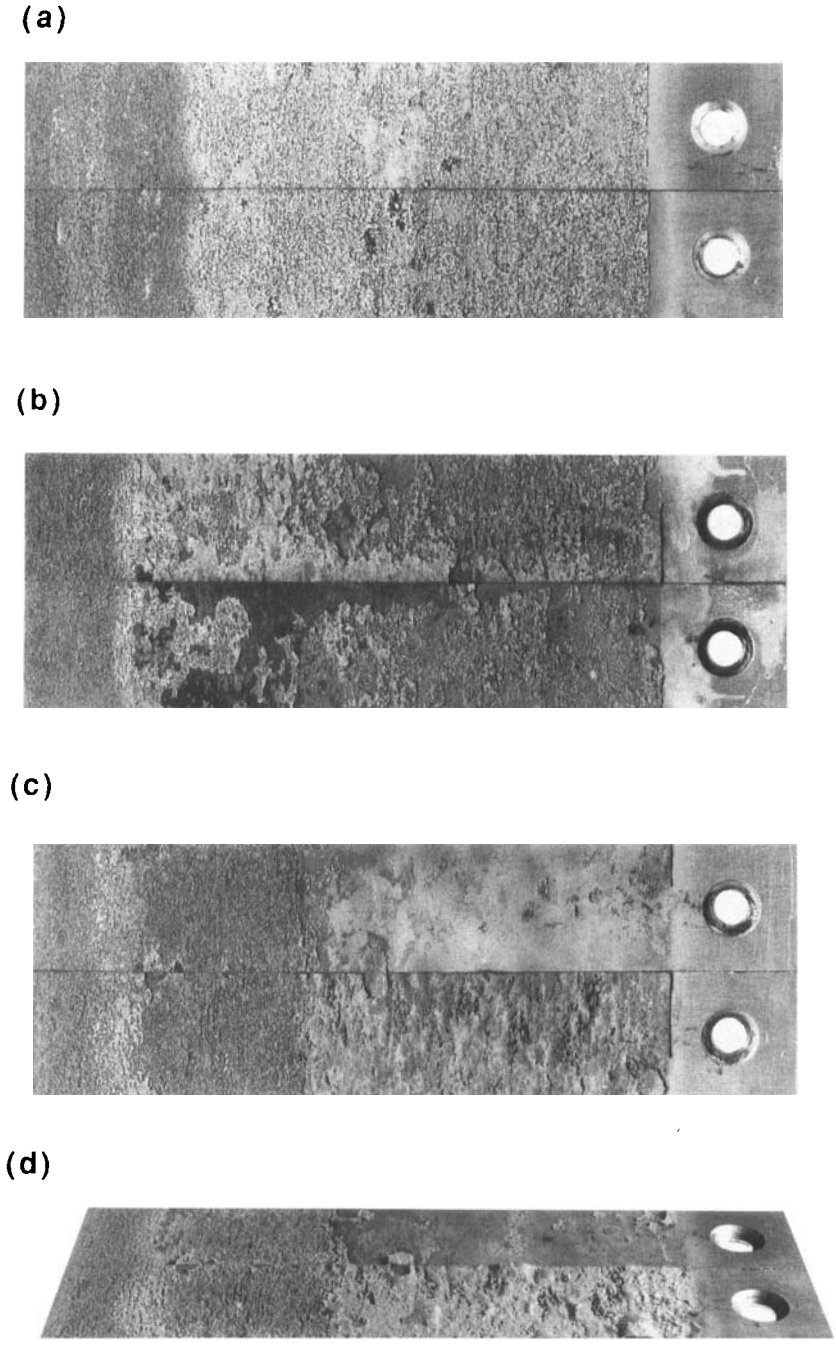

FIGURE 6 Photographs of three fracture surfaces between adherends with a grit-blast plus SCA treatment and tested as follows:

(a) warm dry air, $dw/dt = 0.36$ mm/hr.
(b) warm humid air, $dw/dt = 0.36$ mm/hr.
(c) warm humid air, $dw/dt = 0.036$ mm/hr.
(d) warm humid air, $dw/dt = 0.036$ mm/hr showing plastic expansion of the adhesive.

fracture surfaces shown in Figures 6(a) and 6(b) are both of specimens tested at a *dw/dt* of 0.36 mm/hr. These photographs show that the mode of failure in warm humid air is different from that in dry air. The MAF in warm humid air at a *dw/dt* of 0.36 mm/hr was approximately 0.4 and distributed between the two adherends, typically in zones of 0.5 to 200 mm^2; *i.e.* much larger than for the dry case. A substantial fraction of the surface with "metallic" appearance was stained by water exposure. Near one edge of this specimen, the "metallic" region was almost continuous and largely confined to one adherend. The failed adhesive had expanded plastically. This mode of failure clearly relates to the ingress of water into the bond during the test.

Figure 5, curve (ii), shows that in warm humid air the MAF was 0.5 where *dw/dt* was less than 0.1 mm/hr. Figure 6(c) shows that this failure was mainly confined to one adherend surface. Figure 6(d) shows plastic expansion of adhesive on the mating adherend. This test was terminated at a crack length of approximately 70 mm; *i.e.* where the appearance of the fracture surface had changed to indicate cohesive fracture.

Figure 5 also shows that "adhesive" failure does not necessarily imply greatly reduced fracture toughness. At a *dw/dt* of 0.08 mm/hr, the MAF of 0.5 indicated complete "adhesive" failure, whilst the G_1 of 1300 Jm^{-2} was approximately 70% of the maximum value obtained in warm dry air.

Specimens prepared with a grit-blast plus SCA treatment and tested at a *dw/dt* of 0.3 mm/hr show that instantaneous G_1 was insensitive to humidity (Figure 7). However, a decrease in *dw/dt* to 0.1 mm/hr leads to a decrease in G_1 upon humidification. The new equilibrium takes approximately 2 hours to be reached. Instantaneous G_1 was

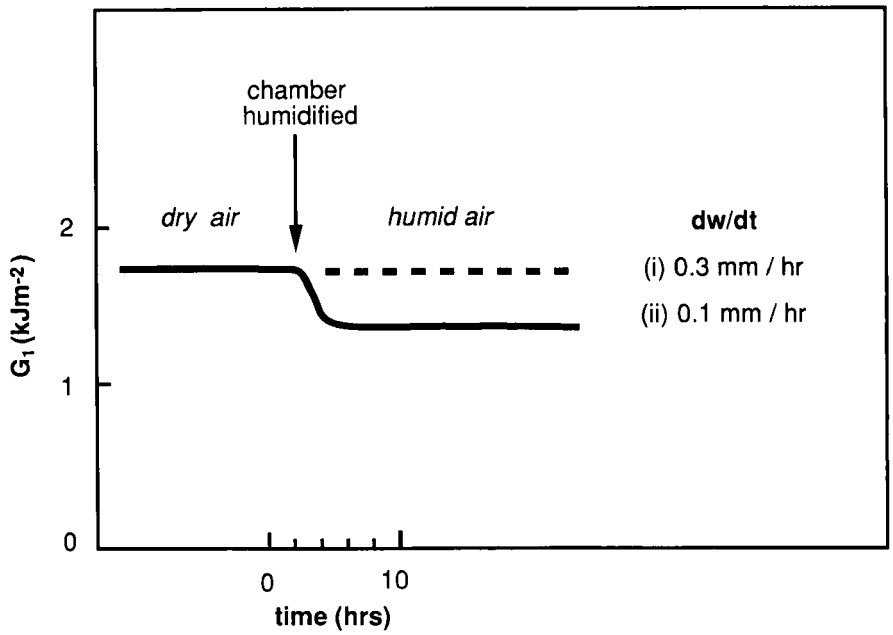

FIGURE 7 Plots of G_1 *versus* time for two values of *dw/dt* for adherends with a grit-blast plus SCA treatment showing the effect of humidity.

calculated in Figure 7 by direct substitution of w and P in equation (1). The values of G_1 used in Figure 5 were calculated from the gradient of a plot of w *versus* P^{-2}. The threshold of load-point displacement rate where G_1 decreases is shown in Figure 7 as approximately 0.3 mm/hr. This is consistent with that shown in Figure 5.

The composition of the fracture surface was obtained by X-ray photoelectron spectroscopy (XPS) with a depth resolution of approximately two to ten atomic layers.[13] The silicon in the SCA molecule was used as a marker for indicating the locus of fracture. Figure 8(i) shows the X-ray photoelectron spectrum from a "metallic" area on the fracture surface of the specimen shown in Figure 6(a); *i.e.* tested in dry air at a dw/dt of 0.36 mm/hr. The presence of both silicon and aluminium in the spectrum indicates that both SCA and aluminium oxide are present. This suggests that the fracture had occurred at the interface containing aluminium oxide, SCA and the adhesive. Figure 8(ii) shows a second spectrum from a "metallic" area on a specimen tested in warm humid air at the same dw/dt. In this case, the absence of silicon in the spectrum indicates that fracture had occurred in the aluminium oxide on the adherend. Analysis of complementary regions of mating adherends support these conclusions.

3.3 Adherends with a Grit-blast plus PAA Treatment

Figure 9, curve (i), shows a plot of G_1 *versus* dw/dt for tests conducted in warm humid air on specimens where the adherends were grit-blasted and then treated with PAA. Water

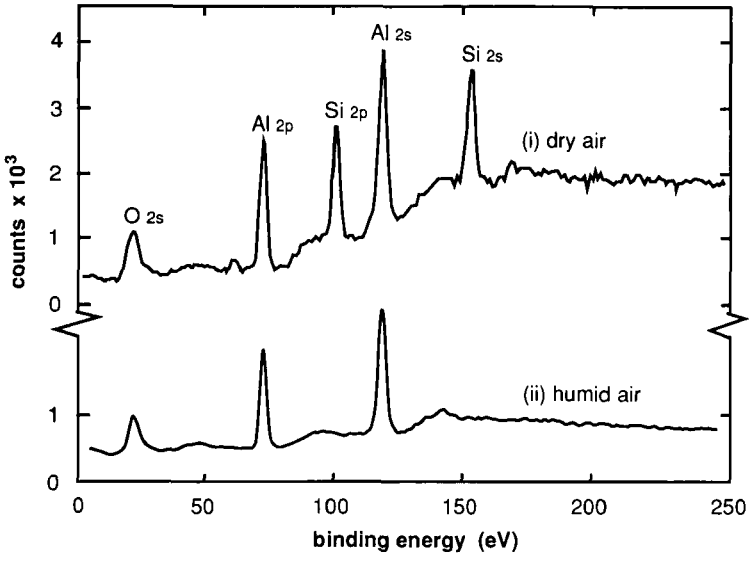

FIGURE 8 X-ray photoelecton spectra of regions with "metallic" appearance on the fracture surfaces of specimens with a grit-blast plus SCA treatment and tested as follows:

(i) warm dry air, $dw/dt = 0.36$ mm/hr (as in Figure 6 (a)).
(ii) warm humid air, $dw/dt = 0.36$ mm/hr (as in Figure 6(b)).

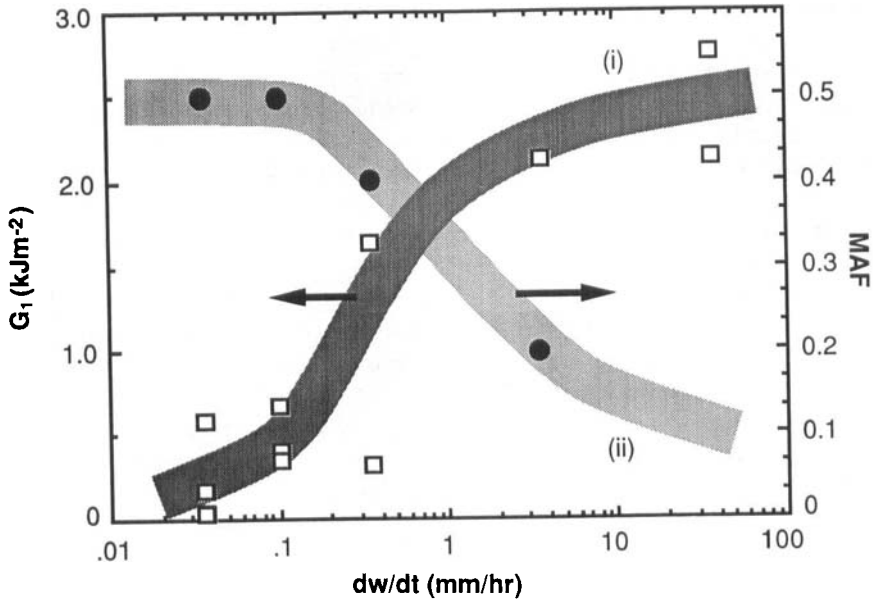

FIGURE 9 Plot of (i) G_1 and (ii) MAF *versus* dw/dt for specimens with grit-blast plus PAA treated adherends, tested in warm humid air. The arrows indicate the relevant reference scale.

vapour caused a large reduction in G_1 where dw/dt ranged between 10 and 0.036 mm/hr, whereas the nominally-dry case showed only a small reduction.

Figure 10(a) shows the fracture surfaces of a specimen tested at 3.6 mm/hr in warm dry air. Again, failure had principally occurred in the adhesive film. Inspection of several specimens indicated that the MAF ranged between 0.05 and 0.2 and was distributed on both adherends in small zones, typically less than 0.5 mm^2. Close inspection of the fracture surfaces revealed that this MAF was mainly due to small voids in the adhesive. There was no evidence of plastic expansion of the adhesive. Failure was cohesive in all dry tests where dw/dt ranged from 36 to 0.085 mm/hr.

Figure 9, curve (ii), shows that the MAF in warm humid air had increased as dw/dt was decreased from 36 to 0.1 mm/hr. Figure 10(b) shows that the fracture surfaces on specimens tested in warm humid air at a dw/dt of 3.6mm/hr were similar to those of specimens tested in warm dry air at the same dw/dt (Figure 10(a)). However, in the humid case, a thin, almost continuous region of "metallic" appearance" was observed near both edges of the specimen. Tearing of the adhesive had occurred in some areas. Figure 10(c) shows that failure was "adhesive" and confined to one adherend surface in a warm humid air test where dw/dt was less than 0.1 mm/hr. Plastic expansion of the adhesive was not observed.

In Figure 9, the MAF increased over the same range of dw/dt as G_1 decreased. This contrasts with the behaviour of the MAF following the grit-blast and the grit-blast plus SCA treatments where a MAF of 0.5 does not necessarily imply a greatly-reduced fracture toughness.

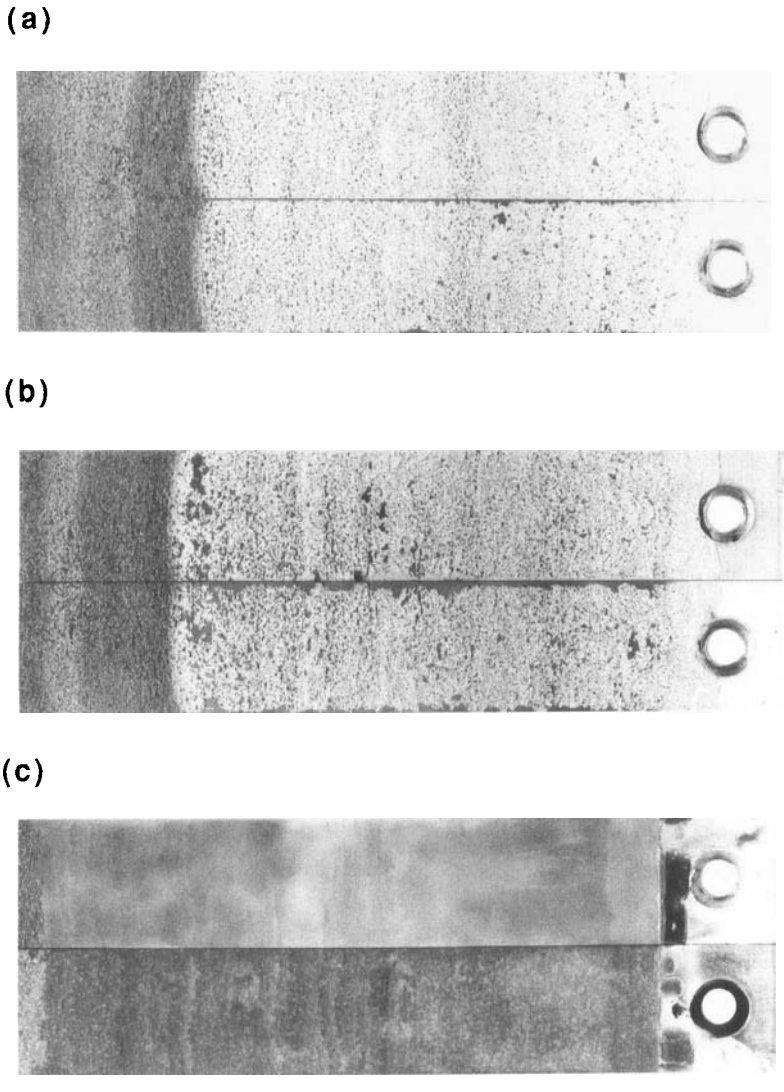

FIGURE 10 Photographs of three fracture surfaces between adherends with a grit-blast plus PAA treatment and tested as follows:

(a) warm dry air, $dw/dt = 3.6$ mm/hr.
(b) warm humid air, $dw/dt = 3.6$ mm/hr.
(c) warm humid air, $dw/dt = 0.1$ mm/hr.

4 DISCUSSION

The elastic energy release rate, G_1, was sensitive to dw/dt in warm humid air, for specimens with grit-blasted adherends[4] (Figure 3, curve (i)) or, to dl/dt (Figure 2). This sensitivity to dw/dt depends strongly on adherend surface treatment (Figure 3(i), 5(i)

and 9(i)). G_1 is replotted against dl/dt in Figure 11 to show the comparison of G_1 with surface treatment.

4.1 Critical Fracture Energy G_{1c}

The G_1 values for all three surface treatments obtained from tests conducted in dry air were essentially the same as values obtained at high crack velocity in humid air as shown in Figure 11. Here, G_1 is equivalent to the critical fracture energy of the undegraded bond, G_{1C}. In dry air, the failure is apparently cohesive for all three surface treatments (Figures 4(a), 6(a) and 10(a)). However, G_{1C} was lower for the grit-blast and the grit-blast plus SCA treatments than for the grit-blast plus PAA treatment (Figure 11). This can be explained in terms of adhesion efficiency. For the grit-blast and grit-blast plus SCA treatments, the MAF was approximately 0.25 (Figures 4(a) and 6(a)) and this translates to approximately 50% adhesion efficiency. The MAF of approximately 0.05 to 0.2 for the grit-blast plus PAA treated adherends, shown in Figure 10(a), indicates that adhesion efficiency is between 90% and 60%. The ratio of the respective bonding efficiencies was between 1.8 and 1.2. The ratio of G_{1C} for the grit-blast plus PAA to G_{1C} for the grit-blast (or the grit-blast plus SCA) treatment is in the range between 1.6 and 1.3 which is similar to the ratio of bonding efficiencies.

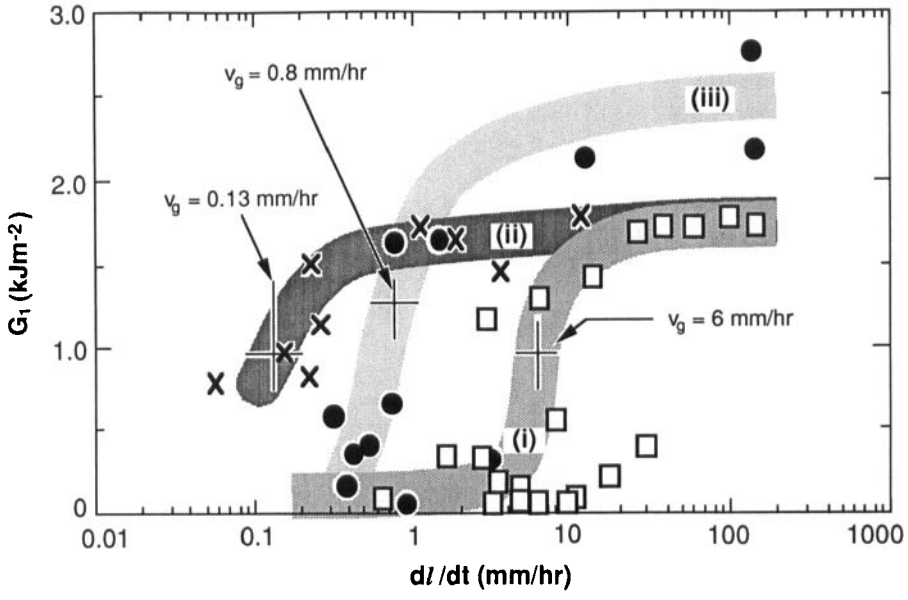

FIGURE 11 Plots of G_1 *versus* dl/dt for three surface treatments:

(i) grit-blast only.
(ii) grit-blast plus SCA.
(iii) grit-blast plus PAA.

Tests conducted in humid air.

The SCA does not improve the mechanical properties of the interface between the grit-blasted surface and the epoxy adhesive when tested at high values of dw/dt (Figure 11(i) and (ii)). Since the SCA does not modify the adherend surface texture, it is suggested that the density of successful atomic bonds with SCA is similar to the density of available atomic bonds without SCA. Examination of the X-ray photoelectron spectrum in Figure 8(i) shows that fracture occurred at the interface containing the SCA. Thus, organic contaminants and/or zones of weak oxide film on the adherends probably limit the dry fracture toughness of the adhesive bond. The role of organic contaminants and/or zones of weak oxide film on the fracture toughness is to be investigated further.

The PAA treatment was shown to improve the interfacial mechanical properties of the undegraded bond (Figure 11). This improvement could be related to the density of successful atomic bonds between the adhesive and the adherend. The PAA treatment used commercially, changed the topography of the surface[10,11,12] and possibly reduced its contamination. Both of these effects would increase the density of successful atomic bonds. Mechanical interlocking between the epoxy adhesive and the micro-porous anodic oxide could also contribute to higher fracture toughness.

4.2 Fracture Energy G_{1SCC}

The fracture energy of a fully-degraded bond, G_{1SCC}, can only be determined at very low crack velocity (Figure 2). In these tests, the lower limit of dw/dt was approximately 0.01 mm/hr and this was sufficiently low to evaluate G_{1SCC} for the grit-blast treatment only. G_{1SCC} was not evaluated for the grit-blast plus PAA, or the grit-blast plus SCA treatments, as the lower plateau in the plot of G_1 *versus* dl/dt was not reached (Figure 11). A multiple displacement-rate test is being developed to determine G_1 at several discrete values of displacement rate in one test of a single specimen. This will reduce the time required to evaluate G_1over a wide range of dl/dt.

4.3 Bond Durability

A graphical mean crack velocity, v_g, is shown in Figure 11. This graphical method was chosen because the transition region for the grit-blast plus PAA and grit-blast plus SCA treatments did not extend to sufficiently low crack velocities for v_{trans} to be calculated. This v_g approximates v_{trans} and is sensitive to the adherend surface treatment in humid air. In these tests, v_g is 6, 0.8 and 0.13 mm/hr for the grit-blast, grit-blast plus PAA and grit-blast plus SCA treatments respectively. The ratio of v_g for one adherend surface treatment to v_g for a reference treatment is used to define a relative durability factor (RDF). Comparing a grit-blast plus SCA treatment with a grit-blast treatment alone, gives an RDF of approximately 50. This implies that the SCA retards degradation of the bond by an approximate factor of 50. Similarly, the grid-blast plus PAA treatment retards bond degradation by a factor of approximately 9 relative to the grit-blast treatment alone. The RDF is imprecise and care must be exercised in its interpretation for service applications. The RDF is not necessarily representative of service conditions, as the CDRT is an accelerated test.

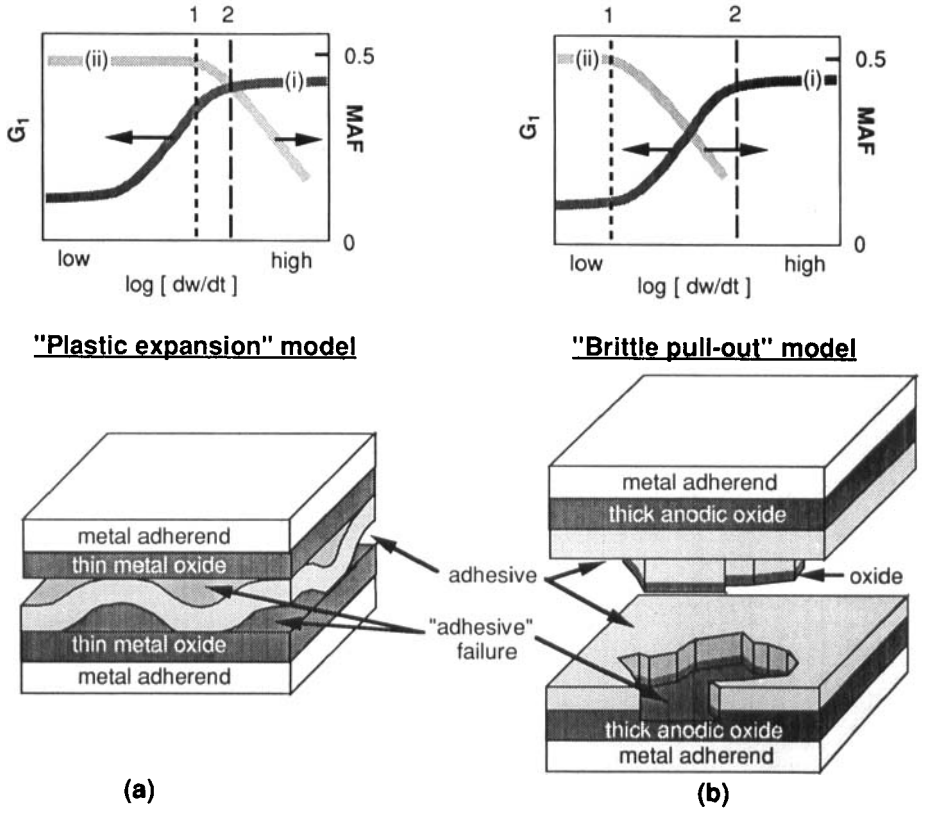

FIGURE 12 (a) A summary of Figures 3 and 5, and the "plastic expansion" model of fracture for grit-blast and grit-blast plus SCA treatments. (b) A summary of Figure 9 and the "brittle pull-out" model of fracture for the grit-blast plus PAA treatment.

Forced separation of the adherends (Figure 4(b), 6(b) and 10(b)) indicated negligible bond degradation ahead of the crack front. Thus, water vapour diffusion from a humid atmosphere to the unstressed specimen edges did not appear to degrade the bond. The diffusion of water vapour into the stressed adhesive near the crack front is, therefore, believed to be the principal cause of bond degradation. The variation in severity of degradation and the associated discolouration along the edges of the fracture surfaces shown in Figures 4(b), 6(b) and 10(b) are believed to be due to variations in the state of water acting within the cracking region. Water in the liquid state is expected to provide more severe bond degradation than water vapour. The variation in severity of degradation shown on the fracture surfaces in Figures 4(b), 6(b) and 10(b) could also explain the decade range in crack velocity where the transition in G_1 occurred.

Figure 11 shows that bond durability is improved by the SCA or PAA treatments. Thus, bond degradation appears to be controlled at the interface where the SCA or PAA treatments have modified the adherend surface:

(i) The SCA treatment provides the best durability of the three adherend treatments. X-ray photoelectron spectra of "metallic" areas on the fracture surfaces of a specimen tested in warm humid air at a dw/dt of 0.36 mm/hr, indicated that fracture had occurred in the oxide film (Figure 8). This dw/dt corresponds to a threshold of weakening in the bond (Figures 5 and 7). Apparently, the SCA inihibits the interaction between the water vapour and the oxide on the adherend surface. It is unlikely that the thin SCA film will influence the interfacial diffusion rate of water vapour significantly[14]. This suggests that competition for bonding sites on the oxide surface between the SCA and water may slow the hydration rate of the oxide. The fact that the SCA is adsorbed onto the adherend from a 1% aqueous solution, strongly suggests that the thermodynamics of adsorption favour the SCA in preference to water. These issues need further investigation.

(ii) The durability of bonds formed on adherends anodized in phosphoric acid is reported to be due to the presence of a phosphate layer on the anodic film[10,11,15]. This textured oxide film has "fingers" which are vulnerable to degradation by water vapour but the phosphate layer is expected to reduce the rate of degradation. Complete adhesive failure along one face (Figure 10(c)) could be due to a "zipper" style failure at these fingers.

4.4 Bond Failure Models

The CDRT shows that total "adhesive" failure does not necessarily imply greatly reduced fracture toughness (Figure 12 (a)). For the grit-blast and grit-blast plus SCA treatments, the load-point displacement rate thresholds for total adhesive failure (*i.e.* MAF = 0.5) were 3.6 and 0.08 mm/hr, respectively (Figures 3 and 5). However, G_1 had only decreased by 20% of the maximum at these load-point displacement rates. Examination of the fracture surfaces showed that areas of the adhesive had expanded plastically (Figures 4(b), 4(c), 4(d), 6(b), 6(c) and 6(d)). This plastic expansion suggests that areas of firm attachment on the adherend linked by compliant adhesive could have distributed the stress to neighbouring attachment areas as shown in the "plastic expansion" model of Figure 12(a). This strongly suggests that preferential degradation of the bond had occurred. The grit-blast and grit-blast plus SCA treatments appear to create both areas of good interfacial durability and areas of comparatively poor durability. The SCA treatment may enhance the protection of those areas of good interfacial durability or may increase the coverage.

It could be argued that very small fragments of adhesive on fracture surface regions having "metallic appearance" could contribute to load transfer. However, the intensity of aluminium peaks in the X-ray photoelectron spectra for SCA treated adherends (Figure 8) suggests that hydrocarbon overlayers are on average less than a few atomic layers thick. Thus, the contribution of such small fragments of adhesive to load transfer is considered to be negligible.

By contrast, the grit-blast plus PAA treatment resulted in the fracture toughness decreasing over the same range of load-point displacement rate where the increase in the fraction of "adhesive" failure had occurred (Figures 9 and 12(b)). Examination of the fracture surfaces showed that the fracture was relatively brittle (Figures 10(b)

and 10(c)). This behaviour is consistent with both the "zipper" style failure described above and the "brittle pull-out" model shown in Figure 12(b). The small regions of severely degraded bond along the edges of the specimen shown in Figure 10(b) showed evidence of plastic expansion, but this represented only a small fraction of the total fracture area. The associated slight plastic deformation in the adhesive shown in Figure 10(b) is consistent with localised differential bond strength as described in Figure 12(a).

The specimens with grit-blast and grit-blast plus SCA treated adherends showed similar fracture as described by the "brittle pull-out" model of Figure 12(b) when tested in dry air. The MAF of 0.25 ± 0.05 indicated the presence of localised areas of relatively poor adhesion. The topography of the grit-blasted surface, the distribution of contaminants on this surface and inhomogeneities in the oxide film could each account for zones of differential bond strength.

4.5 Limitations of Durability Estimates

The durabilities of bonds estimated with the CDRT appear to be at variance with those obtained by Baker[1,2], using the Boeing wedge test. The details of the surface treatments used by Baker were similar, but not identical, to those described here. This could account for the differences in results. However, the details of the testing procedure could equally explain these differences. Baker's method estimates bond durability from G_1 measurements taken at times of 0 and 48 hours. The elapsed time of 48 hours may be insufficient to ensure complete degradation of the bond by water vapour for the more durable treatments. The relative G_1 values determined with the CDRT at an arbitrary crack velocity of 2 mm/hr would also rank bond durabilities in the order: grit-blast plus PAA, grit-blast plus SCA and grit-blast alone (Figure 11(a)). At this crack velocity, bonds prepared with the PAA and SCA treatments are not fully degraded by water vapour, whereas bonds prepared with a grit-blast alone are. The CDRT also provides critical information on the fracture toughness of bonds exposed to both dry and humid air.

5 CONCLUSIONS

1. The constant displacement-rate test has provided sufficient control over the crack velocity to measure the environmental degradation rate of adhesive bonds.
2. The results of tests indicated that phosphoric acid anodization of a previously grit-blasted surface provided higher fracture toughness in an undegraded bond than surfaces treated with either a grit-blast alone or a grit-blast plus SCA.
3. Tests have also indicated that bonds prepared on adherends treated with grit-blast plus SCA are more durable than those prepared on adherends treated with grit-blast plus PAA. Both of these bonds are more durable than those prepared with a grit-blast treatment alone.
3. Bond failure models relating mechanical properties with fracture surface characteristics have been established using the constant displacement rate test.

6 Acknowledgements

The authors gratefully acknowledge discussion with and contributions from Dr. A. A. Baker and Dr. R. J. Chester. The authors also acknowledge constructive comments from the referees of this paper.

References

1. A. A. Baker, *Composites*, **18**, 293 (1987).
2. A. A. Baker, in *Bonded Repair of Aircraft Structures*, A. A. Baker and R. Jones, Eds. (Martinus Nijhoff Publishers, 1988), p. 122.
3. D. R. Arnott and M. R. Kindermann, Proceedings of The Australian Aeronautical Conference 1989, Melbourne, 9–11 Oct 1989, pp. 192–196.
4. D. R. Arnott and M. R. Kindermann, *J. Adhesion* (in press).
5. "Standard Test Method for Adhesive-Bonded Surface Durability of Aluminium (Wedge Test)," ASTM-D3762-79 (ASTM, Philadelphia).
6. J. A. Marceau and E. W. Thrall, in *Adhesive Bonding of Aluminium Alloys*, E. W. Thrall and R. W. Shannon, Eds. (Marcel Dekker, N. Y., 1985), pp. 177–197.
7. S. Mostovoy, P. B. Crosley and E. J. Ripling, *J. Mater.* **2** (3), 661 (1967).
8. M. H. Stone and T. Peet, "Evaluation of the Wedge Test for Assessment of Durability of Adhesive Bonded Joints," Royal Aircraft Establishment Tech Memo, Mat 349, July 1980.
9. R. G. Schmidt and J. P. Bell, *Adv. Polymer Sci.* **15**, 33 (1986).
10. D. A. Hardwick, J. S. Ahearn and J. D. Venables, *J. Mater. Sci.* **19**, 223 (1984).
11. J. D. Venables, *J. Mater. Sci.* **19**, 2431 (1984).
12. J. A. Marceau, in *Adhesive Bonding of Aluminium Alloys* (E. W. Thrall and R. W. Shannon, Eds. (Marcel Dekker, N.Y., 1985), pp. 51–74.
13. M. P. Seah and W. A. Dench, *Surface and Interface Anal.* **1**, 2 (1979).
14. N. G. Farr, D. R. Arnott, A. N. Rider and H. J. Griesser, Proceedings of The Australian Aeronautical Conference 1989, Melbourne, 9–11 Oct 1989, pp. 216–220.
15. G. D. Davis, T. S. Sun, J. S. Ahearn and J. D. Venables, *J. Mater. Sci.* **17**, 1807 (1982).

NOMENCLATURE

CDRT	Constant displacement-rate test.
G_1	Elastic energy release rate (crack extension force).
G_{1C}	Critical fracture energy of the undegraded bond.
G_{1SCC}	Critical fracture energy of the fully-degraded bond.
w	Load-point displacement.
dw/dt	Load-point displacement-rate.
P	Load.
h	Adherend thickness.
b	Width of adherends.
E	Young's modulus of the adherends.
l	Effective length of the cantilevered adherends.
dl/dt	Crack velocity.
v_{trans}	Transitional crack velocity for estimating bond durability.
v_g	Graphical mean crack velocity for estimating bond durability.
SCA	Silane coupling agent.
PAA	Phosphoric Acid Anodization.
RDF	Relative Durability Factor.
MAF	Metallic Appearance Fraction.